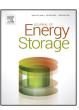
ELSEVIER

Contents lists available at ScienceDirect

Journal of Energy Storage

journal homepage: www.elsevier.com/locate/est



Kinetic study of low temperature capacity fading in Li-ion cells



Jan Patrick Singer*, Kai Peter Birke

Electrical Energy Storage Systems, Institute for Photovoltaics, University of Stuttgart, Pfaffenwaldring 47, 70569 Stuttgart, Germany

ARTICLE INFO

Article history: Received 8 February 2017 Received in revised form 3 July 2017 Accepted 4 July 2017 Available online 23 July 2017

Keywords:
Chemical diffusion coefficient
Activation energy
Activation factor
Lithium-ion cells
Capacity fade
Low temperature
Pseudo-OCV

ABSTRACT

Lithium-ion cells show a reversible capacity fade at low C-rates (C/10) at temperatures below $T=0\,^{\circ}C$. This phenomenon cannot solely been explained by temperature induced impedance raise and the formation of solid electrolyte interphases any more. We investigate four different cell chemistries at temperatures T=25, 0, -10 and $-20\,^{\circ}C$. All measurements are carried out on full cells. The activation energies and especially the ratio of anodic and cathodic activation energies have the highest impact on capacity fading at low C-rates. For quantification of the ratio, we define an activation factor between anodic and the cathodic activation energies. We derive temperature and activation energy behavior on basis of the Butler–Volmer equation for increasing internal voltages and polarization. High activation energies causes high energy demand for activation polarization and an earlier reach of cut-off voltages. If the negative and positive electrode are well balanced with respect to activation energies, the internal voltages which are induced at electrodes boundary layers (electrochemical double layer) are small and the pseudo open circuit voltages lower.

© 2017 Elsevier Ltd. All rights reserved.

1. Introduction

Lithium based secondary battery cells are most common in stationary storages as well as mobile applications. Lithium batteries benefit from higher power and energy densities, lower self-discharge rates as well as higher lifetimes compared to other electrochemical energy storage systems and have opened a variety of applications due to these advantages [1]. However, the performance of all lithium cells stringently depend on the operating temperature. Most applications require a stable operation in temperature range between T = -20 °C and T = 60 °C. Due to safety issues like thermal runaway or accelerated aging processes, the behavior above room temperature $(25 \,{}^{\circ}\text{C} \leq T \leq 60 \,{}^{\circ}\text{C})$ is well known and analyzed [2]. Unfortunately, the low temperature behavior is problematic and still not fully understood. At low temperatures, lithium batteries show a reversible capacity fade. The low temperature power performance, which means high Crates (10 s peak current at C > 10, e.g. as starter battery) has often been investigated. Zhang, Xu and Jow detected the capacity fade due to increasing charge transfer resistance R_{ct} at decreasing temperatures for a cell with lithium nickel-based mixed oxide cathode and graphite anode. R_{ct} is linked to the kinetics of the electrochemical reactions [3].

Therefore, the capacity fades due to a voltage drop by internal resistance increase results in an faster approach of the voltage limits. Up to now, for *C*-rates >1 highly reduced ionic conductivity is determined as the main reason for capacity fading [4].

However, we observe a capacity fade even at pseudo-open circuit voltage (OCV) measurements (C/10) which cannot be explained by decreasing ionic conductivity as a main reason. Fan and Tan [5] discuss the influence of solid diffusion of charge carriers inside the graphite as the ultimate rate limiting factor. Nevertheless we see a capacity fade also for cells with lithiumtitanate (LTO) anodes where a fast two phase reaction mechanism is present. A difference between LTO and graphite is that a solid electrolyte interphase (SEI) is formed on the surface of the graphite because the potential of lithiated graphite is close to Li metal, while the LTO has a potential of around 1.5 V vs. Li/Li⁺ which will make the formation of an SEI more unlikely. Lück and Latz present the theory of reactions at electrified interfaces, especially the adsorption layer in the electrochemical double layer between electrolyte and electrode [6]. This is the prominent mechanism for charge transfer at the polarized interfaces at low temperatures and needs to be described as a two step mechanism.

In this paper, we focus on a method to investigate temperature induced capacity fade in lithium-ion cells without in-depth electrode materials characterization. Our research shows that differences in anodic and cathodic activation energies cause capacity fading at low temperatures due to polarization of the electrodes. Not only those differences, but also high activation

^{*} Corresponding author.

E-mail address: jan.singer@ipv.uni-stuttgart.de (J.P. Singer).

energies have an impact on polarization. These effects induce an increase of internal potentials due to limited kinetics of charge carriers which results in increasing pseudo-OCVs. Limited kinetics occurs as simultaneous phenomena at the electrodes/electrolyte interphases and the solid diffusion in the electrodes. Both lead to increasing polarization voltage $\Delta\phi$ that can be quantified in full battery cells.

2. Experimental

Table 1 shows the investigated battery cells with their cathode and anode materials, nominal voltage $U_{\rm N}$, end of charge voltage $U_{\rm EC}$, end of discharge voltage $U_{\rm ED}$ as well as nominal capacity $C_{\rm N}$. For the low temperature induced capacity fading studies, we used four different lithium based secondary battery cells with the most common anode materials graphite (Li_xC) for cell (a) and (b) and lithium-titanate (Li_xTi_5O_{12}) for cell (c) and (d). The cathode materials are for (a) lithium nickel cobalt aluminum oxide (NCA), for (b) and (c) lithium iron phosphate (Li_xFePO_4) and (d) lithium manganese oxide (Li_xMn_2O_4). All cells are either commercial or tailor-made. Since we intended to carry out an nondestructive method for battery cells characterization, detailed knowledge about the materials composition is not a prerequisite. By choosing a low C-rate, the influence of different cell geometries, especially the cells winding and I or stacking, is assumed to be negligible.

We measure pseudo-OCV curves for determining the capacity fade at low temperatures with A CTS lab cell tester by BaSyTec. It is used as voltage/current source, for temperature logging and data recording in time-steps of $\Delta t = 1$ s. A constant current (CC) $I_{\rm C} = C_{\rm N}/10$ charges the cell until the voltage reaches $U_{\rm EC}$, followed by t = 1 h of relaxation time and vice versa for discharge until $U_{\rm ED}$.

A Binder MK 53 climate chamber holds the cell environment at constant temperatures with an accuracy of $\Delta T = \pm 0.5$ K. To receive a benchmark for comparing capacity fades, every cell is characterized at T = 25 °C, T = 0 °C, T = -10 °C and T = -20 °C. A second cell of every type is characterized as reference to exclude manufacturing defects and measurement errors.

Cyclic voltammetry (CV) supplies electrochemical data in order to receive information for the full cells electron transfer kinetics. For every cell chemistry, we determine a optimal scan rate ν for CV. Optimal ν means the best compromise between measuring time and minimum time step within the measurement system can deliver the current response. A Gamry Reference 3000 potentio-stat/galvanostat measures the CV within the defined temperatures.

Additionally, we observe particle morphologies by using a scanning electron microscopy (SEM) in post-mortem surface analysis. The distribution of particle size is determined by measuring particle surface cross section using ImageJ software.

3. Results and discussion

3.1. Pseudo-open circuit voltage

Fig. 1(a)–(d) shows the pseudo-OCV measurements of the four cells (a)–(d) within the voltage limits according to Table 1. Fig. 1(a)

Table 1 Investigated battery cells with corresponding cathode material, anode material, nominal voltage $U_{\rm N}$, end of charge voltage $U_{\rm EC}$, end of discharge voltage $U_{\rm ED}$, nominal capacity $C_{\rm N}$ and cell type.

• • • • • •		
(1) A 3-12 A 1-4	(b) (c)	Cylindrical Cylindrical Pouch Prismatic

shows NCA cell chemistry for charging with respect to the left axis and discharging (right axis) over normalized usable capacity $\frac{C_p}{C_N}$ while C_p is the practical capacity at the corresponding temperature T. C_N is investigated by measuring the charge transfer during discharge at $T=25\,^{\circ}\text{C}$ with $I_D=C/10$ current, C_p at the according temperature T and charge direction.

In charge direction, normalized usable $\frac{C_p}{C_N}$ fades compared to $T=25\,^{\circ}\text{C}$ (green line) with decreasing temperature. At $T=0\,^{\circ}\text{C}$ (blue line) 87.52%, at $T=-10\,^{\circ}\text{C}$ (red line) 76.46% and at $T=-20\,^{\circ}\text{C}$ (black line) 51.81% of initial capacity is usable.

The capacity fading is on the one hand side caused by lower ionic conductivity which results in an increase of the internal resistance [3,7,4]. However, at very low *C*-rates (pseudo-OCV) the effect of the lower ionic conductivity does not dominate. Basically, an increasing internal resistance can be observed at a higher potential. We consider the characteristics at $T = 25 \,^{\circ}\text{C}$ and $T = 0 \,^{\circ}\text{C}$ of Fig. 1(c) in charging direction. The blue line ($T = 0 \,^{\circ}\text{C}$) is almost on the same charge voltage level as the green one ($T = 25 \,^{\circ}\text{C}$). When it reaches U_{EC} , there is a gap $\Delta \frac{C_{\text{P}}}{C_{\text{N}}}$ between $T = 25 \,^{\circ}\text{C}$ and $T = 0 \,^{\circ}\text{C}$ which represents the capacity fade while the resistance does not increase.

This phenomenon happens in case of all four chemistries in Fig. 1(a)–(d) in charging as well as discharging direction. Fig. 2 shows $\frac{C_p}{C_N}$ at T = 25, 0, -10 and -20 °C for charging and discharging. $\frac{C_p}{C_N}$ follows Kohlrauschs stretched exponential function for describing polarization which is used for curve fitting since we assume, the low temperature behavior is a polarization effect of the electrodes. Fig. 3 shows a discharge characteristics of a lithium-ion cell. We can determine three main regions to describe losses in a cell characteristics [8]. The ohmic losses influence the slope and level of the plateau in the middle part. Losses in mass transport influence the voltage drop at Depth of Discharge DoD near one. For the observed phenomena, we investigate the region of activation polarization at DoD close to zero.

3.2. Post-mortem analysis

Figs. 4(a)–(d) and 5 (a)–(d) show post-mortem analysis by scanning electron microscope (SEM) images and particle size distributions for the electrodes. Fig. 4(a)–(d) shows surface cross sections of the cathodes and Fig. 5(a)–(d) for the anodes. The particle distributions follow a logarithmic normal distribution, which is common for describing pulverized materials [9]. The capacity fading decreases with wider particle size distributions of the cathode materials.

Cathode (d) shows the highest distribution width and the best low temperature performance, while sample (c) has the smallest particles and the worst performance. However, this correlation is not observable for the anodes.

By using the particle size distribution and the geometrical size of the electrodes $A_{\rm e}$ it is possible, to estimate the contact area S between electrodes surface and electrolyte. For simplification, Rui et al. estimate this contact area as the same area as geometrical area of the electrodes [7]. We assume that the active material particles are spherical segments. Half of the surface of the segments are in contact with the electrolyte as shown in Fig. 6. The particle radius r is used to calculate the spherical surface by $A_{\rm s} = 2\pi r^2$. Since we know the relative frequency h of particle sizes, we calculate a correction factor for the active surface $f_{\rm S} = \sum_{n=1}^{50} h_n A_{\rm s.n.}$. Taking into account, that the spherical estimation is an approximation, we use the calculated contact area S only for relative comparisons:

$$S = A_{\rm e} f_{\rm S} \tag{1}$$

Download English Version:

https://daneshyari.com/en/article/5127326

Download Persian Version:

https://daneshyari.com/article/5127326

<u>Daneshyari.com</u>